

Seismic strengthening applied to heritage: an experimental study on rubble stone masonry walls

Reforço sísmico aplicado ao património:
um estudo experimental em alvenarias de pedra ordinária

Madalena Ponte

Rita Bento

Andrea Penna

Abstract

The seismic assessment and rehabilitation of heritage masonry buildings is a complex task, that requires great prior research work, especially for the most innovative strengthening solutions, such as FRCM systems. Thus, twelve rubble stone masonry with hydraulic lime mortar specimens representative of traditional buildings of the centre-south region of Portugal and the Mediterranean countries were built. Different strengthening techniques were applied to the specimens, considering the requirements for interventions in historic buildings related to their authenticity, promoting minimum intervention, and ensuring the compatibility and durability of the materials. Furthermore, the frequent existence of frescoes/tiles in the interior conditions the application of the strengthening to only one side of the wall. Hence, FRCM systems with glass and carbon meshes were studied on only one side of the specimen. The main experimental results of quasi-static cyclic tests obtained through envelope curves, in terms of resistance and deformation capacity, are presented here.

Resumo

A avaliação e reabilitação sísmica de edifícios patrimoniais em alvenaria é uma tarefa complexa que requiere um largo trabalho de investigação prévio, especialmente para soluções de reforço mais inovadoras, como os sistemas FRCM. Assim, foram construídos doze espécimes de alvenaria de pedra ordinária e cal hidráulica representativos dos edifícios tradicionais da região centro-sul de Portugal e dos países mediterrâneos. Diferentes técnicas de reforço foram aplicadas aos espécimes, considerando os requisitos para intervenções em edifícios históricos relativos à sua autenticidade, promoção da mínima intervenção, e assegurando a compatibilidade e durabilidade dos materiais. Ainda, a frequente existência de frescos/azulejos no interior condiciona a aplicação do reforço a apenas um lado da parede. Assim, sistemas FRCM com malhas de vidro e carbono foram estudados apenas num lado dos espécimes. Os principais resultados dos ensaios cíclicos quase-estáticos obtidos através das curvas envolventes, em termos de resistência e capacidade de deformação, são aqui apresentados.

Keywords: Rubble stone masonry / Quasi-static cyclic tests / Seismic strengthening / FRCM system / Heritage rehabilitation

Palavras-chave: Alvenaria de pedra ordinária / Ensaios cíclicos quase-estáticos / Reforço sísmico / Sistema FRCM / Reabilitação do património

Madalena Ponte

CERIS
Instituto Superior Técnico
Universidade de Lisboa
Lisboa – Portugal
madalenaponte@tecnico.ulisboa.pt

Rita Bento

CERIS
Instituto Superior Técnico
Universidade de Lisboa
Lisboa – Portugal
rita.bento@tecnico.ulisboa.pt

Andrea Penna

Department of Civil Engineering and Architecture
University of Pavia
andrea.penna@unipv.it

Aviso legal

As opiniões manifestadas na Revista Portuguesa de Engenharia de Estruturas são da exclusiva responsabilidade dos seus autores.

Legal notice

The views expressed in the Portuguese Journal of Structural Engineering are the sole responsibility of the authors.

PONTE, M. [et al.] – Seismic strengthening applied to heritage: an experimental study on rubble stone masonry walls. **Revista Portuguesa de Engenharia de Estruturas**. Ed. LNEC. Série III. n.º 17. ISSN 2183-8488. (novembro 2021) 23-30.

1 Introduction

The study of strengthening interventions in heritage masonry buildings is complex and requires certain care. Masonry is a highly heterogeneous material, difficult to characterize, and, therefore, the performance of a high number of experimental tests is necessary for its reliable characterization. In Portugal, there are few experimental studies on rubble limestone masonry walls with lime mortar, typically used in the centre-south region of Portugal and the Mediterranean countries, such as [1] and [2]. Also, other experimental campaigns were carried out to characterize other types of typical Portuguese masonry ([3], [4]).

More recently, to combat the incompatibility of materials, the use of fibre-reinforced composite meshes (such as FRCM systems) is becoming more popular instead of steel meshes with cement coating. The FRCM retrofit method has been proved by several experimental tests to improve mechanical properties and deformation capacity of masonry elements; however the majority of the studies in the literature are for brick masonry, while only a few are for stone masonry ([5], [6], [7], [8], [9]), that is the most common material in the southern Europe monuments.

This paper aims to provide some lights regarding the experimental in-plane behaviour of typical ancient Portuguese rubble limestone masonry when reinforced with FRCM systems using glass or carbon meshes.

2 Test specimens and materials

Six $120 \times 120 \times 40$ cm³ specimens of rubble stone walls representative of ancient Portuguese monuments were built in the Structures and Strength of Materials laboratory (LERM) of Instituto Superior Técnico Structures (Figure 1) to assess their behaviour under quasi-static cyclic shear tests. After the walls were dry (minimum 28 days), strengthening solutions with Glass- or Carbon-FRP mesh and lime-based binder (GFRCM/CFRCM system) were applied. Each solution was applied to two specimens, being in total: 2 walls unreinforced (URM 1 and URM 2), 2 walls with GFRP system (G 1 and G 2), and 2 walls with CFRP system (C 1 and C 2). The FRCM system was applied only on one side of the specimens, as is the case of many historic buildings due to the frequent presence of mural paintings on the walls.

To portray the current state of ancient masonry walls existent in Portuguese monuments, the specimens were built with several voids inside and were tested after a minimum period of 4 months after its construction to ensure the mortar's hardness.

The materials used were provided by company SECIL (<https://secilpro.com>), one of the main cement, aggregates and mortars producing companies in Portugal. The specimens were built with roughly cut limestones, the most common stone used in ancient monuments and buildings surrounding Lisbon, and natural hydraulic lime mortar – REABILITA CAL CS (compression strength class CS II, following EN 1015-11 [10]). Natural hydraulic lime mortar is an innovative binder, the result of a research and development process by SECIL group, which allows a use compatible with old substrates and presenting a behaviour that meets the rigorous requirements of today.



Figure 1 Construction of the masonry specimens at LERM, IST

3 Strengthening techniques and materials

The mortar used to help fixing the FRP meshes to the substrate is suitable for the technique and based on a natural hydraulic lime mortar – REABILITA CAL FORCE (compression strength $> 14 \text{ N/mm}^2$, following EN 998-1 [11]). Regarding the application of the FRCM systems, the glass FRCM system (GFRCM) applied is marketed by SECIL group, while the carbon FRCM system (CFRCM) is marketed by the company S&P Clever Reinforcement Ibéria. Both meshes are bi-directional. The glass mesh used is named REABILITA REDE AR 160, with openings of $40 \times 40 \text{ mm}$ and a weight of 160 g/m^2 . The connectors used in the GFRCM system are applied by pressure and a second layer of a grid with smaller openings was added in a reduced area around the connectors (approximately 20 cm in each direction) to help distribute concentrated stresses (Figure 2, on the right).

The carbon mesh used is named S&P ARMO-mesh 500/500, with openings of $17 \times 17 \text{ mm}$ and a weight of 374 g/m^2 . The connectors used in this system are also made of carbon fibres with a length to distribute the concentrated stresses of approximately 20 cm (Figure 2, on the left).



Figure 2 Application of carbon- (left) and glass- (right) FRCM systems on specimens

The application of the FRCM systems was the same for both glass and carbon meshes, varying only in its anchoring system, and followed the codes [12] and [13]. The total thickness of the strengthening solutions applied to the specimens was around $3/4 \text{ cm}$. As this study intends to evaluate a masonry panel representative of historic buildings, the ends of the grids were not



mechanically fixed to the wall, concrete beam, and/or concrete footing, since in many real cases this is not possible to perform (either due to stone edges, or even the impossibility of removing the pavement stones). Connectors are approximately spaced 50 cm from the nearest connector, giving a total of 5 connectors per wall. It is worth noting that the holes for connectors were always drilled in the stones.

4 Quasi-static cyclic tests set-up

Quasi-static cyclic tests were performed on all specimens according to [14]. Vertical stress of 0.3 MPa was applied to the specimens based on the actual state of stresses of load-bearing walls in old Lisbon masonry buildings [1], and on the state of stress at the bottom of walls of the chapel of the National Palace of Sintra [15]. Thus, the specimens were first subjected to a vertical pre-compression load, that was kept constant, as much as possible, during the quasi-static cyclic test. The walls were tested with boundary conditions as cantilever systems, fixed at the concrete base and allowing displacements and rotations at the top of the specimen. After the vertical load was applied, the horizontal load was transmitted by a mechanical actuator at the top of the wall through a system of steel plates appropriately connected with steel bars. The set-up is presented in Figure 3.

The first part of the loading protocol followed consists of four cycles until reaching $1/4$ of the maximum horizontal force predicted. Thus, it is possible to characterize the elastic branch of the wall's behaviour. After reaching this point, the horizontal actuator starts to be controlled through horizontal displacement, using a control wire LVDT attached to the concrete beam at the top of the wall. The first pattern of the imposed displacements consists of five single fully reversed cycles at displacements of 1.25% , 2.5% , 5% , 7.5% , and 10% of the ultimate displacement. The second displacement pattern consists of phases, each containing three fully reversed cycles of equal amplitude, at displacements of 20% , 40% , 60% , 80% , 100% , and 120% of the ultimate displacement, with additional increments of 20% until specimen failure. The displacement history of horizontal displacement vs. time was obtained with the control horizontal LVDT.

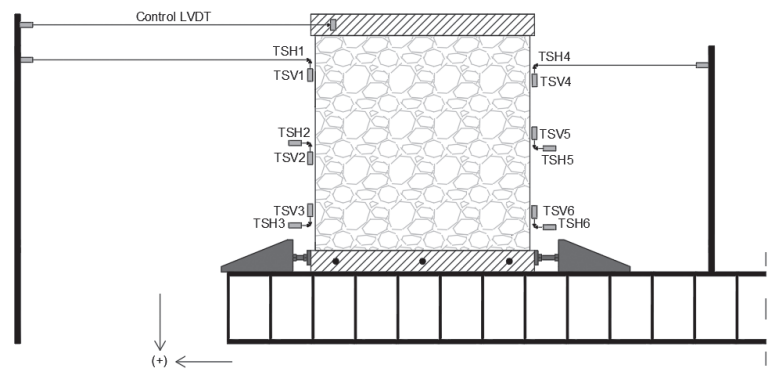


Figure 3 Images of the quasi-static cyclic tests set-up

On each lateral side of the wall, horizontal and vertical LVDT's were placed as close as possible to the top, mid-height, and bottom of the wall, while taking into consideration that the holes to fix the connectors' supports need to be drilled in the stone.

5 Results and discussion

5.1 Force displacement hysteresis diagrams and failure modes

Figure 4 presents the horizontal force-displacement hysteretic curves. The shear force V is the horizontal force exercised by the horizontal actuator on the concrete beam at the top of the wall. δ is the in-plane horizontal drift calculated by dividing the difference of the top horizontal displacement and the displacement at the bottom of the wall, by the total height (from the base until the point of the load application). The envelope curves were defined by considering the value of the force at the first time a displacement is attained in the cyclic curves. Also, in Figure 5 are presented the failure modes of each specimen at the end of the tests. Failure henceforth was defined as the point when a reduction of 20% of the peak load was detected, or when the damage level was so high that the integrity of the wall was at risk.

For both unreinforced walls (URM 1 and URM 2), there is a clear force decay after reaching the peak load. At that stage, the walls were completely damaged with clear diagonal shear cracks at both sides of specimens and the detachment of parts of the walls was on the verge of occurring. The cracks developed along the mortar bed joints.

In the case of the strengthened walls, the weakest part became the connection between the concrete foundation and the wall. Therefore, the first damage to appear for the strengthened walls was always its detachment from the concrete base, which is marked in the envelope curves as the first visible crack. Even though this occurred, it was possible to observe clear improvements in the behaviour of the strengthened walls regarding the unstrengthened ones. Following the detachment of the strengthened walls from

the concrete base, an initial rigid body behaviour with rotation took place for all strengthened walls, without presenting significant strength degradation.

For wall G 1, during the rocking behaviour, diagonal shear cracks started to appear, going through the wall in-depth, immediately followed by the detachment of the lower cornerstones. Only a crack is visible on the side with the strengthening solution, while the majority is located on the facade without strengthening and on the sides. It is also worth mentioning that this is the only wall where damage is visible on the side with strengthening. The early reduction of stiffness on the negative side (pull) of the envelope curve is due to the early detachment of the wall from the concrete base on the left side of the specimen. Even though the extensive damages of G 1, indicating collapse, the specimen did not present strength's decay. The test was interrupted for a drift of about 2.4% due to a possible fall of parts of the wall that were severely damaged.

Wall G 2 presents less damage than G 1, one diagonal shear crack (with a small opening) from corner to corner is visible in the backside of the wall (unstrengthened side). The damage is mostly concentrated in the corners, where toe crushing occurs, and the lower stones got detached. In this wall, it was verified a small decrease of strength and the test was interrupted when 80% of the peak load was attained, exhibiting a higher drift capacity than G 1.

Wall C 1 presents clear damage with several wide diagonal shear cracks in the unstrengthened side of the wall. The test was interrupted before reaching the 20% decay of strength, due to the separation of the two leaves of stone of the wall, causing instability on the wall with a possible out-of-plane collapse.

Lastly, wall C 2 behaves as a rigid body with a typical rocking behaviour. The wall is substantially undamaged with only a few small horizontal cracks at the base corners when a decrease of 20% of the peak load is reached. Furthermore, there is almost no dissipation of energy in the hysteresis diagram.

It is also worth mentioning that, since cracks were only present in the bed joints and no sliding occurred, the hysteresis cycles present in general low energy dissipation and strength degradation.

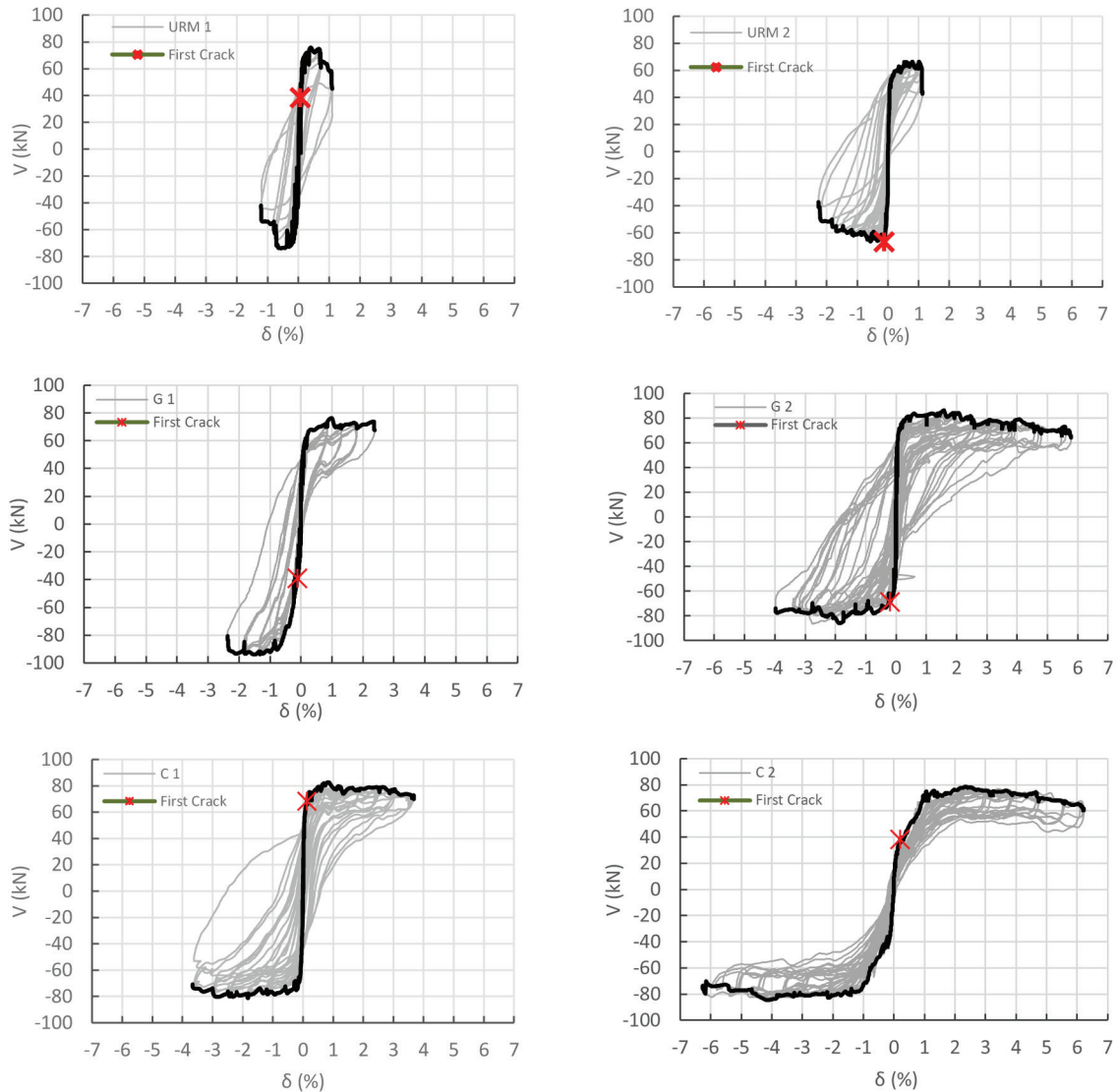


Figure 4 Force-displacement hysteretic and envelope curves

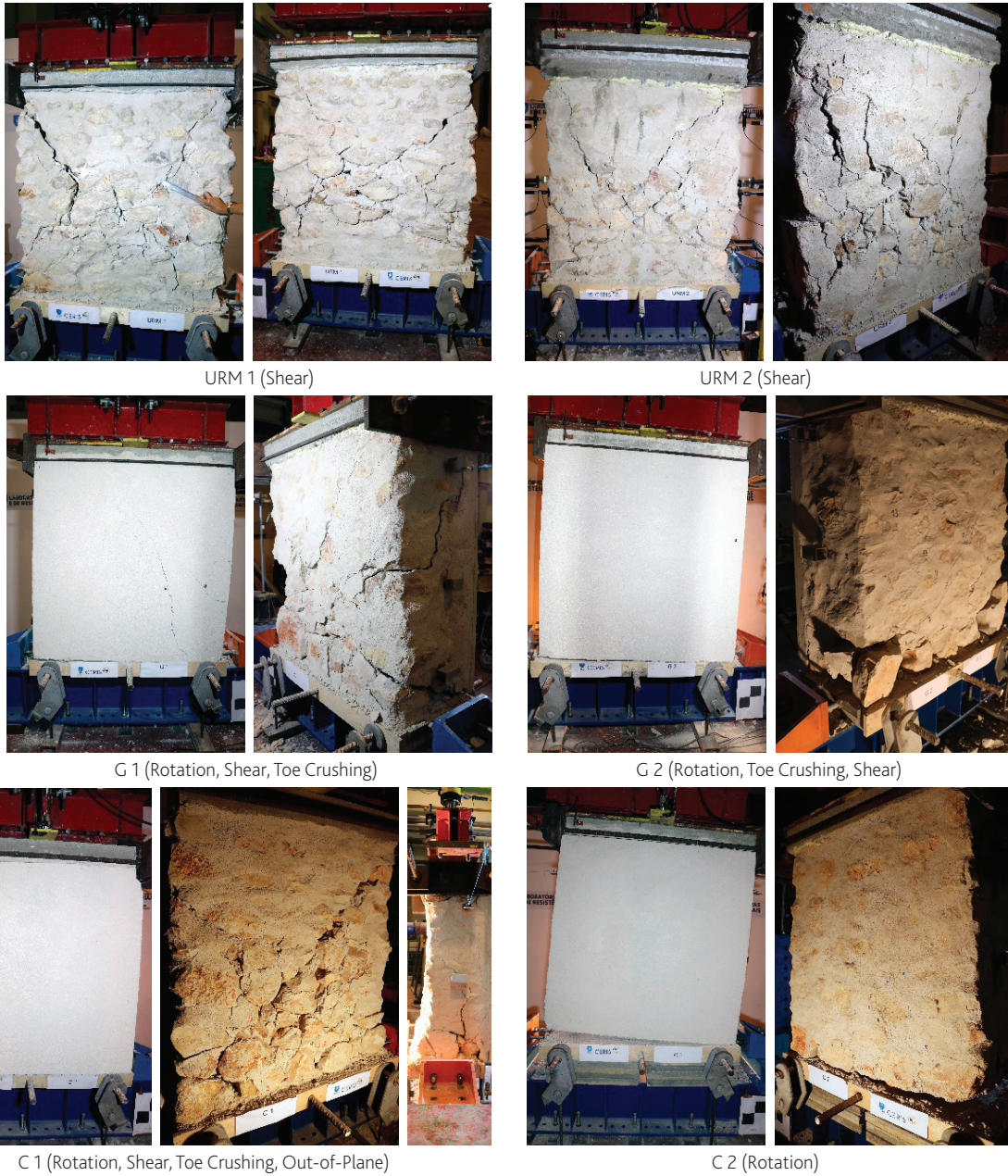


Figure 5 Failure modes at the end of the tests

5.2 Mechanical parameters obtained from quasi-static cyclic tests

The key parameters obtained from the experimental envelop curves are presented in Table 1 and Table 2. It is possible to conclude that the strengthening solution presents almost no influence on the strength capacity of walls since it is only applied on one side of the wall, not causing the confinement of the masonry. However, in terms of seismic vulnerability, it is more interesting to analyse the drift capacity of the strengthened walls. The ultimate drift (δ_u) was defined at the first cycle where a reduction of 20% of the peak load (V_{max}) occurred, or when the test stopped due to imminent detachment of parts of the wall. The ultimate drift of each wall was considered the minimum value between positive (push) and negative (pull) directions, except for wall G 2 because the strength decay occurs in the direction with a higher drift value. Opposite to the load capacity, the ultimate drift of the strengthened walls increases significantly, around 3.4 times for a system with a glass mesh and around 4.2 times with a carbon mesh.

The effective stiffness used in the bilinearization of the envelope curves is the secant stiffness at $0.6 V_{max}$, according to the Italian Standard [16]. No significant influence of the strengthening in the effective stiffness of the masonry walls was found, as this parameter deeply depends on the connection of the wall to the concrete base. For walls URM 1, G 1, and C 2, in which a crack along the base was immediately formed at the beginning of tests, the equivalent stiffness is significantly lower than in the other walls.

The cumulative dissipated hysteretic energy was calculated for each cycle and compared with the corresponding maximum drift, as presented in Figure 6. It is possible to observe that the

unstrengthened walls present higher dissipated energy when compared with the strengthened walls. This was expected due to the shear failure of walls URM 1 and URM 2. On the other side, the dissipated energy for the strengthened walls presents a very similar trend along with the increase of the lateral drift, except for wall C 2 that presents a rigid body behaviour with no damage, as already commented while analysing the hysteretic curves.

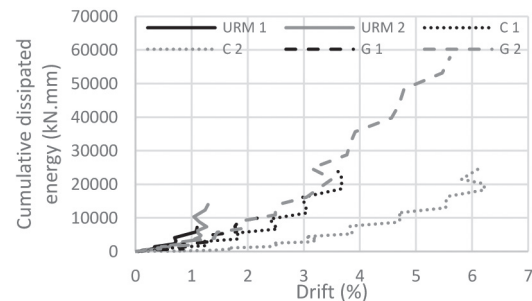


Figure 6 Cumulative dissipative energy of each specimen as a function of lateral drift

6 Conclusions

The results obtained are a first step towards the study of FRM systems in rubble limestone with hydraulic mortar masonry walls. The paper presents the application of the strengthening solutions only on one side of the walls, as in reality, this is very common to occur, not only in monuments, but also in residential buildings, due to its permanent use. Both glass and carbon meshes show a

Table 1 Parameters obtained with quasi-static tests in terms of strength capacity, ultimate drift (δ_u), and effective stiffness

Specimen	Peak load, V_{max} (kN)			Drift at failure (%)			Effective stiffness (kN/mm)			
	Push (+)	Pull (-)	Mean	Push (+)	Pull (-)	δ_u	Mean	Push (+)	Pull (-)	Mean
URM 1	75.8	73.9	70.8	1.0	0.8	0.8	1.2	53.7	111.6	90.0
URM 2	66.8	66.6		1.6	1.5	1.5				
G 1	76.3	94.0	85.7	2.4	2.4	2.4	4.1	95.5	18.5	109.9
G 2	86.3	86.3		5.7	4.0	5.7				
C 1	82.6	81.2	81.8	3.7	3.7	3.7	5.0	97.7	72.5	46.6
C 2	78.7	84.6		6.2	6.3	6.2				

Table 2 The ratio of the properties of strengthened and unstrengthened walls in terms of load capacity, ultimate drift, and effective stiffness

Mean Values	Ratio of properties of strengthened and unstrengthened specimens	
	Peak load	Ultimate drift
GFRM strengthening	1.2	3.4
CFRMC strengthening	1.2	4.2

significant increase of lateral drift capacity, about 3.4 and 4.2 times, respectively. While, in terms of strength and stiffness this is not visible, due to the application of the strengthening only on one side of the wall. Besides the different lateral drift capacity, both mesh materials presented similar results in terms of failure modes, peak load, and dissipated energy as the failure of the walls was controlled by the fragile behaviour of the connection of the masonry walls with the concrete foundation. The differences in stiffness are related to the connection of the wall to the concrete base rather than with the different strengthening solutions.

For further studies, it is interesting to compare the economic aspect of both solutions. While the carbon mesh presents a higher increase of capacity, it is also the most expensive option.

Even though more experimental tests should be carried out, the results here obtained represent a valuable reference for seismic retrofit design purposes.

Acknowledgments

The authors would like to thank SECIL for providing all materials and technicians for the construction of walls and the application of strengthening solutions. In addition, the first author would like to acknowledge the financial support of the Portuguese Foundation for Science and Technology (Ministry of Science and Technology of the Republic of Portugal) through a PhD scholarship [grant number SFRH/BD/145571/2019].

References

- [1] Milosevic, J.; Lopes, M.; Gago, A.S.; Bento, R. (2015) – In-plane seismic response of rubble stone masonry specimens by means of static cyclic tests. *Construction and Building Materials* 82, 9-19. <https://doi.org/10.1016/j.conbuildmat.2015.02.018>
- [2] Milosevic, J.; Gago, A.S.; Lopes, M.; Bento, R. (2013) – Experimental assessment of shear strength parameters on rubble stone masonry specimens. *Construction and Building Materials* 47, 1372-80. <http://dx.doi.org/10.1016/j.conbuildmat.2013.06.036>
- [3] Costa, A.A.; Arede, A.; Costa, A.; Oliveira, C.S. (2011) – *In situ* cyclic tests on existing stone masonry walls and strengthening solutions. *Earthquake Eng Struct Dyn* 40, 449-71. <http://dx.doi.org/10.1002/eqe.1046>
- [4] Vasconcelos, Graça (2005) – Experimental investigations on the mechanics of stone masonry: characterization of granites and behaviour of ancient masonry shear walls, University of Minho, Ph.D. Thesis.
- [5] Ferretti, F.; Incerti, A.; Tilocca, A.R.; Mazzotti, C. (2019) – In-Plane Shear Behavior of Stone Masonry Panels Strengthened through Grout Injection and Fiber Reinforced Cementitious Matrices, no. October. <https://doi.org/10.1080/15583058.2019.1675803>
- [6] Corradi, M.; Borri, A.; Castori, G.; Sisti, R. (2014) – Shear strengthening of wall panels through jacketing with cement mortar reinforced by GFRP grids. *Compos. Part B Eng.* 64, no. August, 33-42. <https://doi.org/10.1016/j.compositesb.2014.03.022>
- [7] Gattesco, N.; Boem, I.; Dudine, A. (2014) – Diagonal compression tests on masonry walls strengthened with a GFRP mesh reinforced mortar coating. *Bulletin of Earthquake Engineering* 13, no. 6, 1703-1726. <https://doi.org/10.1007/s10518-014-9684-z>
- [8] Guerreiro, J.; Proença, J.; Ferreira, J.G.; Gago, A. (2018) – Experimental characterization of in-plane behaviour of old masonry walls strengthened through the addition of CFRP reinforced render. *Compos. Part B Eng.* 148, 14–26. <https://doi.org/10.1016/j.compositesb.2018.04.045>
- [9] Feo, L.; Luciano, R.; Misseri, G.; Rovero, L. (2016) – Irregular stone masonries: Analysis and strengthening with glass fibre reinforced composites. *Compos. Part B Eng.* 92, 84–93. <https://doi.org/10.1016/j.compositesb.2016.02.038>
- [10] CEN. (2019). EN 1015-11: Methods of test for mortar for masonry - Part 11: Determination of flexural and compressive strength of hardened mortar, (January).
- [11] CEN. (2016). EN 998-1: Specification for Mortar for Masonry Part 1: Rendering and Plastering Mortar.
- [12] AC 434–13. 2013 – Acceptance criteria for masonry and concrete strengthening using fabric-reinforced cementitious matrix (FRCM) composite systems. ICC Evaluation Service.
- [13] CNR-DT 215/2018. 2018 – Guide for the Design and Construction of Externally Bonded Fibre Reinforced Inorganic Matrix Systems for Strengthening Existing Structures. CNR – Advisory Committee on Technical Recommendations for Construction, Rome, Italy.
- [14] ASTM E2126 – 11. 2018 – Standard Test Methods for Cyclic (Reversed) Load Test for Shear Resistance of Vertical Elements of the Lateral Force Resisting Systems for Buildings. American Society for Testing and Materials, (Reapproved 2018), 15p. <https://doi.org/10.1520/E2126>
- [15] Ponte, M.; Bento, R.; Costa, A.A. *et al.* (2021) – Reduction of earthquake risk of the National Palace of Sintra in Portugal: the Palatine Chapel. *International Journal of Disaster Risk Reduction*. <https://doi.org/10.1016/j.ijdr.2021.102172> (in press, journal pre-proof)
- [16] Infrastrutture, M. D., & Trasporti, E. D. E. I. 2019 – Circolare n. 35 del 21 Gennaio 2019. Istruzioni per l'applicazione dell'«Aggiornamento delle «Norme tecniche per le costruzioni» di cui al decreto ministeriale 17 gennaio 2018. Roma: IPZS. 337 p. (in Italian)